CERN – PS DIVISION

PS/CA/Note 2000-001
CERN-NUFACT Note 016

ANALYSIS OF DIFFERENT OPTIONS FOR A HIGH INTENSITY PROTON DRIVER FOR NEUTRINO FACTORY

B. Autin, M. Chanel, M. Giovannozzi, M. Martini

Abstract

This note reports a number of different layouts for designing a high intensity proton driver. Such a machine should perform beam accumulation and bunch compression in order to achieve the performance needed for the production of neutrino in the context of a Neutrino Factory.

The different approaches are described in details as well as the optics of the various lattices.

Geneva, Switzerland
14 January 2000

1 Introduction

Among the many possible scenarios for high-energy machines and physics of the post-LHC era [1,2], one is based on the construction of a so-called Neutrino Factory. The neutrino beams are generated by the decay of muon pairs themselves obtained by the decay of pions and kaons. The latter particles are produced by the interaction of a high intensity proton beam onto a production target. In the scheme presently under study at CERN, such a complex may consist of three machines:

- A superconducting linac
- An accumulator ring
- A compressor ring

The superconducting linac is discussed elsewhere [3]. The present note reports on possible design of the two rings involved in the scheme. In Table 1 are summarised the main beam parameters for the three machines [4].

	Parameter	**Unit**	**Value**
Linac output beam characteristics	kinetic energy, T	GeV	2.000
	γ		3.132
	β		0.947
	$\beta\gamma$		2.968
	pulse frequency	Hz	100
	pulse duration	ms	2
	# of μbunch trains		~12 x 600
	pulse intensity	H^-/pulse	$1.2\cdot10^{14}$
	train spacing	ns	276
	#of μbunches/train		15
	μbunch spacing	ns	2.8
	μbunch intensity	H^-/μbunch	$1.2\cdot10^{9}$
	μbunch length	ns	~1
	energy spread (2σ)	MeV	~0.5
	rel. momentum spread (2σ)		$\sim0.2\cdot10^{-3}$
	long. emittance, ε_l	eVs	$0.22\cdot10^{-3}$
	norm. hor. Emittance (1σ)	μm	0.6
	norm. ver. Emittance (1σ)	μm	0.6
Acc.	bunch length (4σ)	ns	50
	rel. momentum spread (2σ)		$1.5\cdot10^{-3}$
	norm. hor. Emittance (1σ)	μm	50
	norm. vert. Emittance (1σ)	μm	50
Comp.	bunch length (4σ)	ns	6
	rel. momentum spread (2σ)		$1.2\cdot10^{-2}$
	norm. hor. Emittance (1σ)	μm	50
	norm. vert. Emittance (1σ)	μm	50

Table 1: Summary of beam characteristics at the output of the Linac, accumulator and compressor ring respectively for the Neutrino Factory complex under study.

In the design of a circular machine a major parameter is its radius of curvature. For the two rings under consideration it has been decided to choose a mean radius of 150 m for each machine. This requirement allows using the tunnel of the ISR machine. Having determined the overall geometry, still two different options are available:

- Isochronous machine. In this case the revolution frequency is not a function of the momentum spread. This means that the slip factor η, defined as

$$\eta = \frac{\Delta T/T}{\Delta p/p} = \gamma_{\mathrm{tr}}^{-2} - \gamma^{-2}$$

  is zero.
- Quasi-isochronous machine. In this case $\eta \neq 0$, but small, namely $|\eta| \leq 10^{-2}$.
- Non-isochronous machine. Similarly $\eta \neq 0$, of the order of $|\eta| \geq 10^{-1}$.

In machines operating at transition no longitudinal space charge effects occur. On the other hand, this is not true for quasi- or non-isochronous rings. In fact, in high-current machines not operating at transition, longitudinal space charge forces induce bunch lengthening and therefore, rf power is needed for compensation. Operating the accumulator ring under a non-isochronous condition (e.g. $\eta = -0.1$) would require a space charge correcting rf voltage of the order of 0.5 MV. This voltage would be lower for a quasi-isochronous accumulator ring.

Unfortunately, various instabilities can arise due to the impedance of the added rf cavities. As an example, a sharp cavity impedance yields long range wake fields which may drive couple bunch instabilities, while a broad impedance yields short range wake fields that can lead to single bunch instabilities.

After accumulation, the bunch compression process has to reduce the bunch length by a factor of about eight before ejection in order to provide the required beam quality for pion production. This process requires a very high rf voltage. Hence, bunch compression must be achieved within a few machine revolutions to avoid the harmful longitudinal space charge effects. This fact imposes to work with the compressor operating under a non-isochronous regime as the larger the slip factor $|\eta|$, the faster the bunch rotation. The very different physical conditions of the beam in the two phases (accumulation and compression) make not feasible to perform both actions in the same ring, the main problem being the beam loading in the high voltage rf system needed to perform the bunch compression. Therefore, the envisaged solution consists of two rings: in the first one a low voltage rf system, say 0.5 MV, runs during the 2 ms accumulation stage, while in the second ring the high voltage rf system, say 8 MV, performs the fast compression stage during few machine revolutions.

To summarise, one can state that the accumulator ring can be an isochronous, a quasi-isochronous or a non-isochronous lattice, while the compressor ring has to be a non-isochronous lattice.

In the rest of this note a number of different lattices will be presented for all these classes of machines.

2 Isochronous (quasi-isochronous) ring

An isochronous machine satisfies the condition $\eta = 0$. This is equivalent to state that the transition energy is $\gamma_{\mathrm{tr}} = \gamma$. Furthermore, it is well known that for a machine

based on a FODO lattice the transition energy is also a function of the horizontal optical parameters through the following approximate relation

$$\gamma_{\mathrm{tr}} \approx Q_{\mathrm{H}} \left[\frac{\mu_{\mathrm{H}} / 2}{\sin(\mu_{\mathrm{H}} / 2)} \right],$$

where $Q_{\mathrm{H}}, \mu_{\mathrm{H}}$ represent the horizontal tune and the phase advance per cell respectively. This fact implies that, when the design energy is quite low (as in the present scenario), the horizontal focusing for a large isochronous machine is rather weak, leading to high beta values and large beam size. The constraint imposed by the choice of the bending radius has a critical effect on the value of the horizontal dispersion function D in the ring. In fact, using the relation for the momentum compaction factor

$$\alpha_p = \gamma_{\mathrm{tr}}^{-2} = \frac{\Delta L / L}{\Delta p / p} = \frac{1}{C} \oint_C \frac{D(s)}{\rho(s)} ds$$

it can be shown that the following expression holds

$$\alpha_p = \frac{1}{C} \sum_{n=1}^{N} \int_{n\mathit{th}\ \mathrm{bend}} \frac{D(s)}{\rho(s)} ds = \frac{1}{C} \sum_{n=1}^{N} \frac{1}{\rho_n} \int_{n\mathit{th}\ \mathrm{bend}} D(s)\, ds$$

since $\rho(s) = \infty$ outside the dipoles and assuming a constant value ρ_n in the n*th* bending magnet. *C* stands for the ring circumference. Thus

$$\alpha_p = \frac{1}{C} \sum_{n=1}^{N} \frac{L_n}{\rho_n} \overline{D}_n = \frac{1}{\overline{R}} \sum_{n=1}^{N} \frac{\theta_n}{2\pi} \overline{D}_n$$

$\overline{R} = C / 2\pi$ being the average radius of the machine, while L_n, θ_n, $\overline{D}_n$ stand for the length, bending angle and mean value of the dispersion function at the location of the n*th* bending magnet, respectively. Using the fact that the sum of all bending angles equals 2π, the mean dispersion over all bending magnets around the ring can be defined as follows

$$\overline{D}_{\mathrm{bends}} = \sum_{n=1}^{N} \frac{\theta_n}{2\pi} \overline{D}_n .$$

Hence

$$\overline{D}_{\mathrm{bends}} = \alpha_p \overline{R}.$$

Therefore, for the case under study, the average dispersion function would be of the order of 15 m. This situation is clearly unacceptable for the compressor ring, where the large value of $\overline{D}_{\mathrm{bends}}$ together with the big momentum spread would make the beam size grow beyond any acceptable limit.

In order to overcome this difficulty, a possible solution consists in introducing a number of dipoles with a negative value of the radius of curvature, in order to lower the value of $\overline{D}_{\text{bends}}$. Let us consider a different situation where *M* extra bends of length *L* are inserted in the lattice, *M/2* with negative (positive) bending radius $-\rho_M$ ($+\rho_M$), respectively. Under the hypothesis that the orbit lengthening generated by the *M* bending can be neglected, then

$$\alpha_p = \frac{\overline{D}_{\text{bends}}}{\overline{R}} + \frac{M\,\theta_M}{4\pi\,\overline{R}}(\overline{D}^{+}_{\text{bends}} - \overline{D}^{-}_{\text{bends}})$$

where $\overline{D}^{+}_{\text{bends}}$ and $\overline{D}^{-}_{\text{bends}}$ stand for the mean dispersion over the dipoles with positive and negative curvature respectively and θ_M represents the deflection angle produced by each additional dipole. Assuming that $\overline{D}^{+}_{\text{bends}} = -\overline{D}^{-}_{\text{bends}} = \overline{D}_{\text{bends}}$, the mean dispersion can be decreased as

$$\overline{D}_{\text{bends}} = \frac{\alpha_p\,\overline{R}}{\left(1 + \frac{M\theta_M}{2\pi}\right)}.$$

From the previous formula, it is apparent that to reduce by a factor two the average value of the dispersion function one should add a number of additional dipoles generating a total deflection angle of π per each group of dipoles.

In case the orbit lengthening cannot be neglected, it is sufficient to modify the previous equations by taking into account the new value of the circumference length, namely $C_M = C + L\,M$ **.** The result is

$$\alpha_p = \frac{\overline{D}_{\text{bends}}}{\overline{R}_M} + \frac{M\,\theta_M}{4\pi\,\overline{R}_M}(\overline{D}^{+}_{\text{bends}} - \overline{D}^{-}_{\text{bends}})$$

where $\overline{R}_M = C_M / 2\pi$. Even in this case it is possible to compute the reduction in the average value of the dispersion function by imposing the condition $\overline{D}^{+}_{\text{bends}} = -\overline{D}^{-}_{\text{bends}} = \overline{D}_{\text{bends}}$, obtaining

$$\overline{D}_{\text{bends}} = \frac{\alpha_p\,\overline{R}_M}{\left(1 + \frac{M\theta_M}{2\pi}\right)}.$$

It is immediately seen that the gain, under the hypothesis of a non-negligible orbit lengthening, is less important than in the previous case. In fact, the increased length of the machine produces an increase of its average radius and this increases the average dispersion.

For the sake of completeness, it is worthwhile mentioning a different approach. In fact, whenever the geometry of the ring is already determined and no modification can be implemented, it is possible to vary the slip factor by simply using quadrupoles (see Refs. [5,6] for more details on the subject). Additional quadrupoles can be used to

perturb the machine optics, in particular the behaviour of the dispersion function, in such a way to trim the value of η at will.

In the following, the approach based on the modification of the ring geometry by means of additional dipoles will be applied to a number of different lattices. All the optics computations reported in the next sections have been carried out by using the *BeamOptics* program [7].

2.1 Plain FODO lattice

The first approach consisted in computing a machine lattice based on a standard FODO cell. The main parameters are listed in Table 2:

950 m ring length	50 FODO cells L_{cell} =19 m $L_{quadrupole}$=2.0 m L_{dipole} =6.4 m	γ_{tr}=3.13 η=-7×10^{-5}	Q_H=3.15 Q_V=2.90	$k_{F,D}$ =±0.0549 m^{-1}

Table 2: Main parameters of the isochronous, thick lens, plain FODO lattice. In all the tables, k stands for the integrated gradient.

It is clearly seen that the horizontal tune is approximately equal to the value of γ_{tr}. The optical functions are shown in Fig. 1. As discussed in the previous section, one obtains that the maximum value of the dispersion function exceeds 17 m, while the average dispersion in the bending magnets is about 15 m.

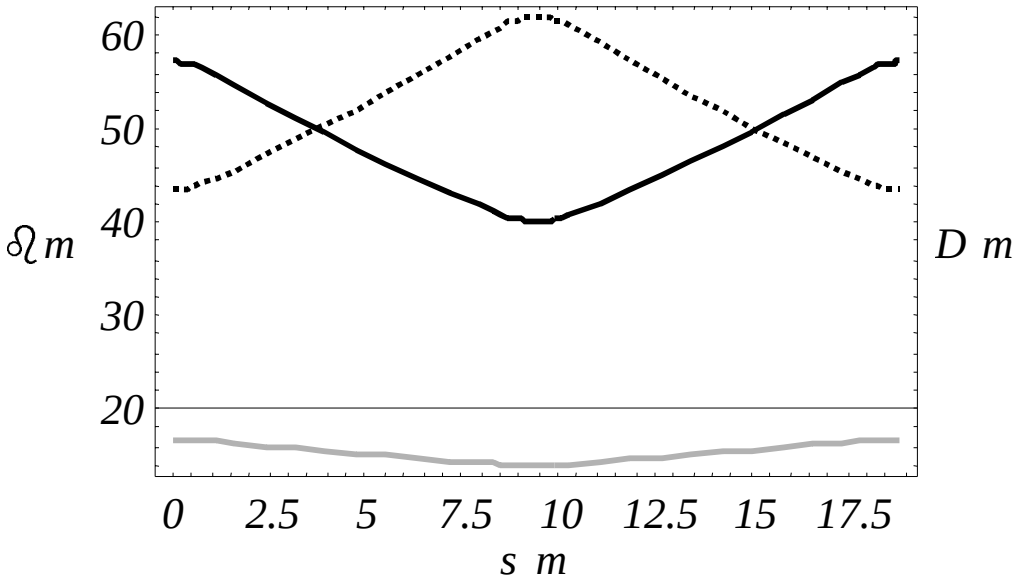

Figure 1: Optical functions and dispersion for the isochronous, thick lens, plain FODO lattice. The continuous black line represents β_H; the dotted line β_V and the light grey the dispersion function.

2.2 LEAR-like lattice

The plain FODO lattice is not the best solution for the compressor ring: in fact, the large momentum spread obtained during the bunch-rotation process, together with the large value of the dispersion function, make the resulting beam size unacceptably

large. An alternative solution consists in looking for a non-FODO lattice. In this case, the LEAR machine [8] and other accumulator rings like the TSR [9] can be used as models for this alternative approach. These machines are also interesting as they optical layout allows to have long straight sections free of magnets.

Those machines are based on a super-period built with two anti-symmetric focussing structures. Every structure consists of a sequence of (FDDF) quadrupoles. In order to obtain such a low value of the transition energy, it is necessary to modify the overall geometry of the super-period by introducing negative-curvature bending magnets. The main bending magnets generate a deflection that is bigger than the one necessary to close-up the machine. Then, additional dipoles are installed at the centre of the super-period to cancel out the excess of bending angle so that the net effect is a closed, although not circular, machine.

The layout of the machine presented in this note consists of sixteen super-periods: this fact allows reducing the bending angle of each magnet thus reducing the magnetic field to be generated. Furthermore, it allows fitting the geometrical constraints imposed by the existing tunnel. The main parameters of the lattice studied are reported in Table 3.

979 m ring length	16 super-periods L_{cell} = 61.2 m $L_{quadrupole}$= 1.0 m L_{dipole} = 5.1 m	γ_{tr}=3.13 η=-7×10^{-5}	Q_H=21.06 Q_V=20.73	k_F = +0.372 m^{-1} $k_{D,1}$= -0.390 m^{-1} $k_{D,2}$= -0.288 m^{-1}

Table 3: Main parameters of the isochronous, thick lens, LEAR-like lattice.

The optical functions are shown in Fig. 2. The dispersion function oscillates around zero and its maximum absolute value does not exceed 7 m, a factor two smaller than for the plain FODO lattice.

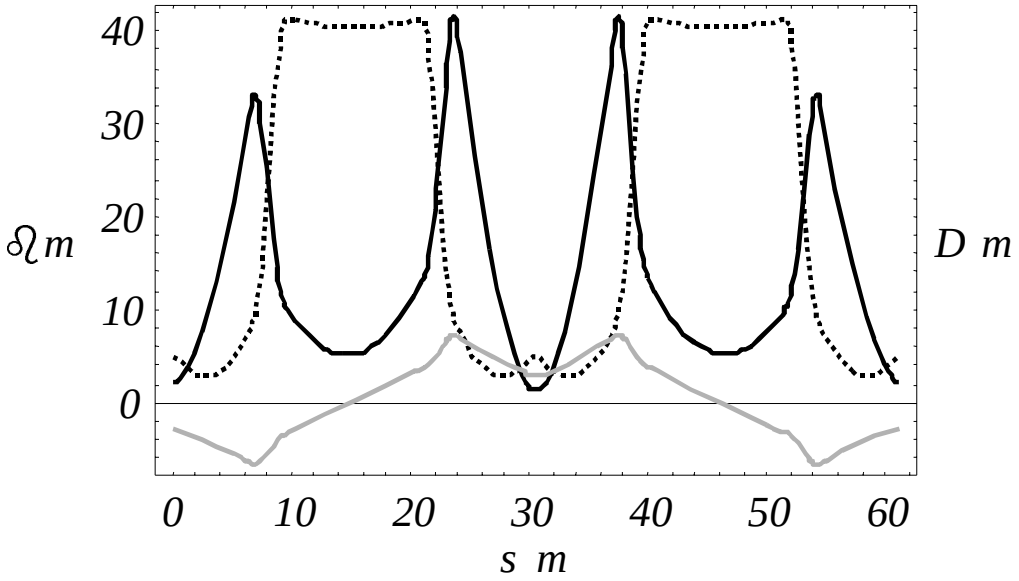

Figure 2: Optical parameters and dispersion of the isochronous, thick lens, LEAR-like lattice. The continuous black line represents β_H; the dotted line β_V and the light grey the dispersion function.

The geometry of a single super-period of the machine is shown in Fig. 3. The two main bending magnets are clearly seen at the two ends of the structure and the two dipoles with negative bending radius at the centre.

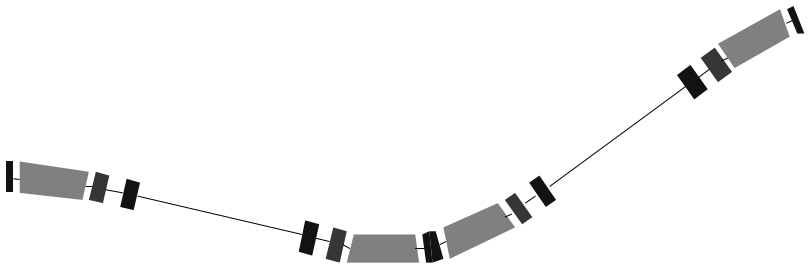

Figure 3: Schematic layout of the super-period of the LEAR-like lattice.

The geometry of the whole ring is reported in Fig. 4. The two circles represent the limits of the existing ISR tunnel.

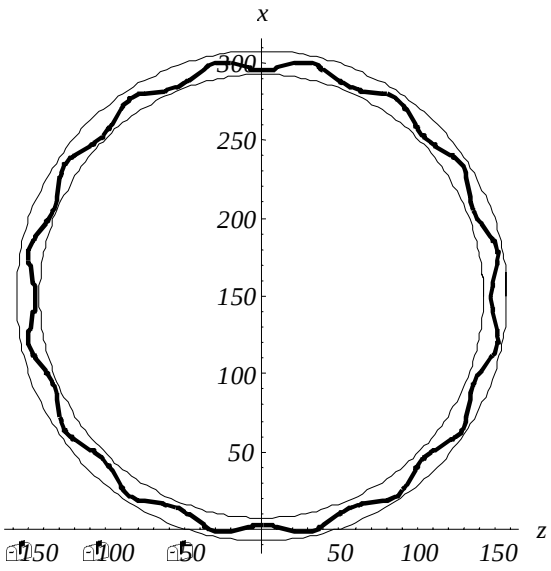

Figure 4: Geometry of the isochronous LEAR-like machine. The inner and outer circles represent the walls of the existing ISR tunnel.

2.3 FODO lattice with wigglers

From the discussion carried out in previous sections, it is clear that dipoles with a negative radius of curvature are necessary to limit the excursion of the dispersion function. A possibility consists in building an optical module based on a FODO cell structure with alternating sign bending magnet so to generate an oscillating behaviour of the dispersion function. It is not trivial to construct such a module, hereafter called wiggler in analogy with the same devices used in electron machines. In order to achieve the isochronicity condition of the ring, the sign of the dispersion within each wiggler must be in phase with the sign of the bending radius to increase the value of the momentum compaction factor (a positive value of the dispersion function should occur in a dipole with a positive bending radius and so forth). It turns out that a solution can be found.

The wiggler cell is three times longer than the nominal FODO cell. It includes five dipole magnets: two at each cell end, two are located at 1/4 L_w and 3/4 L_w respectively, while the last one is placed at 1/2 L_w, where L_w stands for the wiggler's

length. The focusing and defocusing quadrupoles are equally spaced and their relative distance is the same as in the FODO cell. Their gradient is also the same as the FODO cell. Therefore, the underlying principle is that the transverse optical parameters (Twiss functions) are not perturbed by the wiggler structure: the optics of the machine is similar to that of a standard FODO-like ring. On the other hand the propagation of the dispersion function is strongly affected by the presence of the wiggler so that the constraint of the value of the transition energy can be fulfilled. In this way one can achieve the goal of breaking the relationship between the transition energy and the Twiss parameters, while controlling the value of the dispersion function. More details can be found in Ref. [10].

In Table 4 the main parameters of this new layout are summarised:

972 m ring length	8 super-periods 1 FODO + 4 Wigglers L_{cell} = 9.3 m	γt = 3.13 $\eta = -10^{-4}$	Q_H = 42.18 Q_V = 42.18	$k_{F,D} = \pm 0.411\ m^{-1}$ $\mu_{FODO} = 146^o$

Table 4: Main parameters of the isochronous, thin lens, FODO lattice with wigglers.

In Fig. 5 the optical parameters and the dispersion function for one super-period are shown. The beta-functions (horizontal and vertical) behave as in a plain FODO lattice. However, the dispersion function shows a different pattern. The different periodicity with respect to the beta-functions is clearly visible as well as the effect of the negative-curvature bending dipoles.

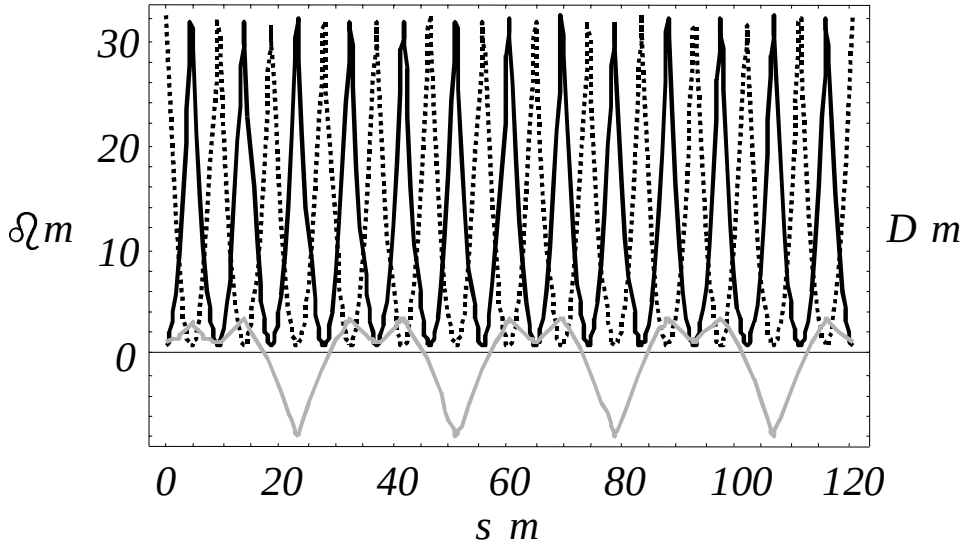

Figure 5: Optical parameters and dispersion of the isochronous, thin lens, FODO lattice with wigglers. The continuous black line represents β_H; the dotted line β_V and the light grey the dispersion function.

Unfortunately, despite many efforts made to further optimise the wiggler cell, it was not possible to find out a configuration for which the dispersion function is more symmetric with respect to the zero value. The drawback of the present solution is that, in order to fulfil exactly the constraint $\eta = 0$, the dispersion has to reach quite big negative

values, whereas it would be much more efficient to increase the maximum positive value while reducing the maximum negative value.

Finally, in Fig. 6 the overall ring geometry is shown. The eight super-periods are clearly visible. The regular FODO cells are located at the position of the eight corners, while the wiggler cells are placed in between FODO structures. The effect of the negative-curvature bending magnets on the machine layout is apparent.

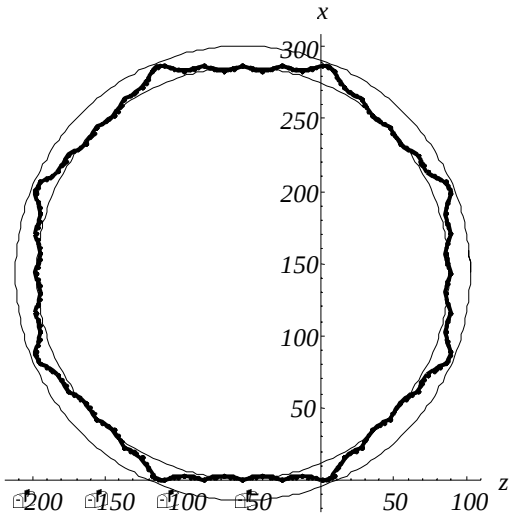

Figure 6 Geometry of the isochronous, thin lens, FODO lattice with negative bending magnets, dispersion suppressors and insertions. The inner and outer circles represent the walls of the existing ISR tunnel.

2.4 FODO lattice with negative bendings, dispersion suppressors and insertions

To conclude the series of isochronous rings, a different isochronous machine is presented. It is based on a FODO lattice with eighteen super-periods. Each super-period includes three FODO cells, two dispersion suppressors, a transition region where the beta-function reduction is carried out and, finally, one shorter FODO cell in the low-beta insertion.

Each dispersion suppressor is based on the same FODO cell used for the regular part of the lattice. To gain space in the straight section, the two bending magnets of the dispersion suppressor cell have been used as free parameters to set to zero the dispersion function and its derivative.

The constraint imposed by the condition $\eta = 0$ requires having some bending magnets of negative-curvature. In Table 5 the main parameters of the lattice are listed.

1098 m ring length	18 super-periods: 3 FODO + 2 Disp.Supp. + 1 FODO (Low-β) L_{cell}= 8.4 m	γ_{tr}=3.13 η=0.0	Q_H=54.47 Q_V=63.49	$k_{F,D}$ = ±0.429 m^{-1} $k^{low\text{-}\beta}_{F,D}$= ±1.159 m^{-1} μ_{FODO} = 128.66°

Table 5: Main parameters of the isochronous, thin lens, FODO lattice with negative bending magnets, dispersion suppressors and insertions.

The rf cavities can be installed in the straight sections: they would benefit from the fact that those sections are dispersion–free. Furthermore, injection and ejection devices could be installed in the low-beta part of the straight sections, thus allowing reducing the aperture needed by the septum and kicker magnets.

The optical parameters for one super-period are shown in Fig. 7. The dispersion function does not exceed the value of 7 m and it shows a rather symmetric pattern with respect to the zero value.

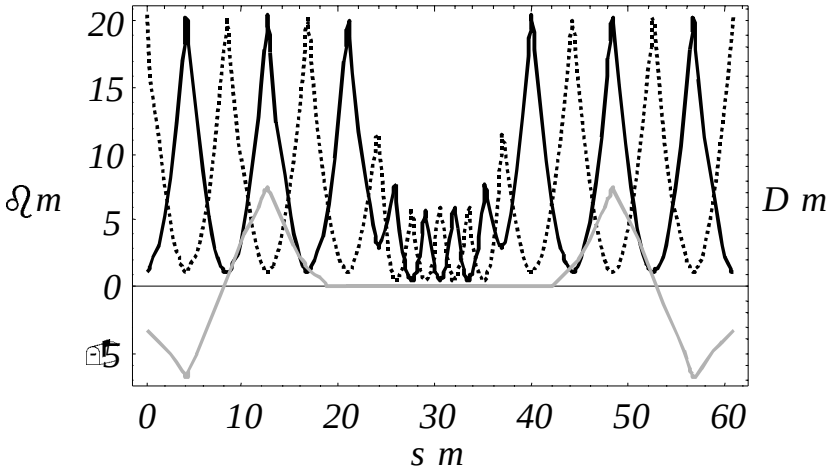

Figure 7: Optical parameters and dispersion of the isochronous, thin lens, FODO lattice with negative bending magnets, dispersion suppressors and insertions. The black line represents β_H; the medium grey β_V and the light grey the dispersion function.

In Fig. 8 the geometry of the ring is reported. The effect of the negative-curvature bending magnet on the overall structure of the ring can be clearly seen.

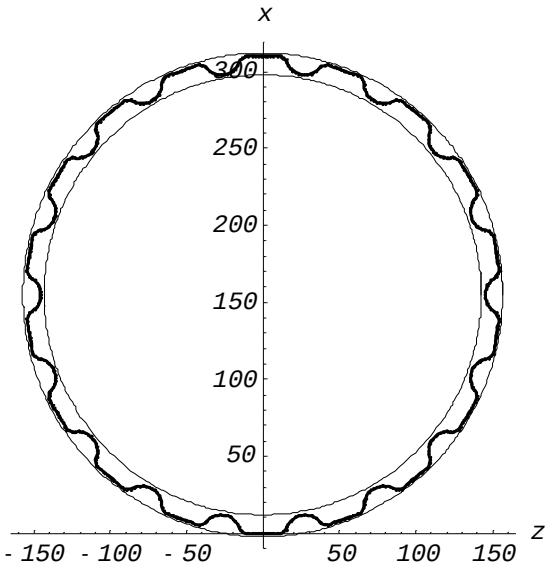

Figure 8: Geometry of the isochronous, thin lens, FODO lattice with negative bending magnets, dispersion suppressors and insertions. The inner and outer circles represent the walls of the existing ISR tunnel.

3 Non-isochronous ring

A completely different solution for the design of the accumulator and compressor rings consists in computing a non-isochronous lattice having $\eta = -0.1$. With this choice and the constraint on the value of the bending radius, it is possible to design a ring without the complexity given by the large amount of bending magnets required by the lattices based on wiggler cells. It is also possible to obtain a well-behaved dispersion function that does not exceed 1 m.

942 m ring length	8 super-periods 5 FODO + 2 Disp.Supp. + 8 FODO L_{cell} =7.9 m $L_{quadrupole}$ =1.0 m L_{dipole} =2.0 m	γ_{tr}=17.95 η=-0.099	Q_H = 25.34 Q_V = 25.45	$k_{F,D}$ =±0.345 m^{-1} μ_{FODO} = 76.35°

Table 6: Main parameters of the non-isochronous, thick lens, FODO lattice with dispersion suppressors and insertions.

This machine consists of eight super-periods. Each super-period is made of 15 FODO cells and it includes a regular part, a dispersion suppressor section and straight sections to be used for injection/extraction. Furthermore, the rf equipment could be installed in the straight sections, together, eventually, with dedicated hardware to perform collimation and halo cleaning. The optical functions are shown in Fig. 9. The dispersion is below 1 m (D_{max}=0.87 m) and the beta-function does not exceed 12.6 m.

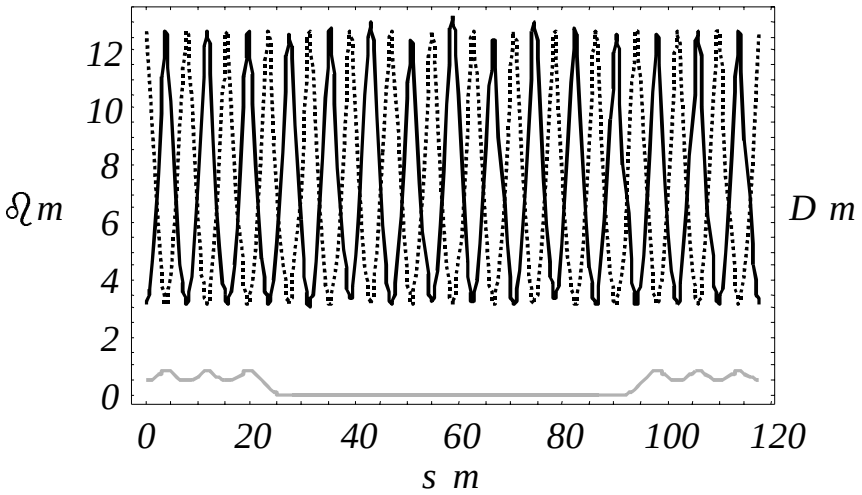

Figure 9: Optical parameters and dispersion of the non-isochronous, thick lens, FODO lattice with dispersion suppressors and insertions. The continuous black line represents β_H; the dotted line β_V and the light grey the dispersion function.

In the straight sections sixteen drifts each 2.9 m long are available for hardware installation (injection/ejection devices, beam instrumentation, rf devices). In addition, the overall geometry has been optimised in such a way that the two rings, the accumulator and the compressor one, can be installed in the same ISR tunnel.

Fig. 10 shows a detail of the superposition of the two rings. The length of the straight section has been chosen so that the crossing occurs in a magnet-free region.

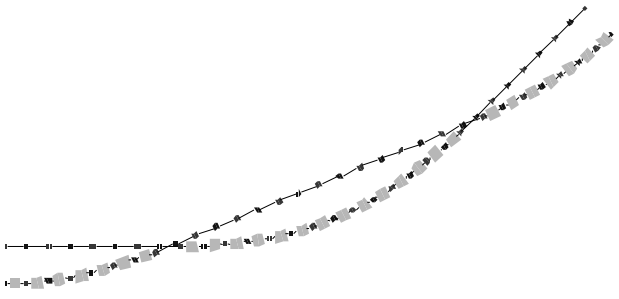

Figure 10: Detail of the crossing of the two rings (accumulator/compressor) based on the non-isochronous machine with FODO lattice.

In Fig. 11, the overall layout of the two rings in the ISR tunnel is presented.

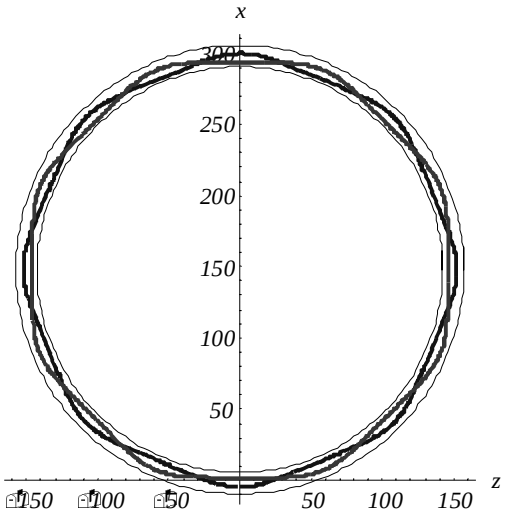

Figure 11: Layout of the two rings (accumulator and compressor) based on the non-isochronous machine with FODO lattice. The inner and outer circles represent the walls of the existing ISR tunnel.

Actually it is also conceivable a different layout where the compressor has a size different than that of the accumulator ring. In this scenario, the twelve bunches are extracted form the accumulator ring in various batches and then injected into the smaller ring to perform the bunch compressor. This second ring could be installed in one of the big experimental caverns in the ISR tunnel. The details of such a variant will be studied in the future.

Conclusions

In this note a number of different solutions have been presented to build a high intensity proton driver for neutrino factory. The different layouts include both isochronous and non-isochronous machines.

The most promising scenario is based on two separated machines: a non-isochronous accumulator and a non-isochronous compressor ring. Both of them can be located into the ISR tunnel. Although, the solution presented in this note foresees the same size for the two rings, another possibility would be to have a small compressor ring to be installed in an experimental cavern of the ISR tunnel.

Acknowledgements

The authors would like to thank the members of the Proton Driver Accumulator Compressor (PDAC) working group, R. Cappi, J. Gareyte, R. Garoby, H. Haseroth, E. Métral, D. Möhl, K. Schindl and H. Schönauer, for many fruitful discussions.

References

[1] J. Ellis, E. Keil, G. Rolandi, *Options for Future Colliders at CERN*, CERN/SL-98-004, 1998.

[2] B. Autin, A. Blondel and J. Ellis eds., *Prospective Study of Muon Storage Rings at CERN*, CERN 99-02, ECFA 99-197, 1999.

[3] R. Garoby, M. Vretenar, *Status of the proposal for a Superconducting Proton Linac at CERN*, CERN/PS 99-064 (RF), NEA Workshop, Aix-en-Provence, France, 22-24 November 1999.

[4] R. Cappi, *private communication*, 1999.

[5] T. Risselada, *An isochronous Optics for EPA*, CERN/PS Note 99-02 (LP), 1999.

[6] T. Risselada, *Isochronicity Adjustments Using Multipoles in Rings and Transfer Lines*, CLIC-Note-405, 1999.

[7] B. Autin, C. Carli, T. D'Amico, O. Gröbner, M. Martini, E. Wildner, *BeamOptics, A PROGRAM FOR ANALYTICAL BEAM OPTICS*, CERN Yellow Report 98-06, 1998.

[8] D. Möhl, *The CERN low energy antiproton ring LEAR*, Proceedings LNS, Gif-sur-Yvette, 521-531, 1983.

[9] E. Jeaschke *et al*., *The Heidelberg Test Storage Ring for Heavy Ions TSR*, in Proceedings of the 1988 European Particle Accelerator Conference, Rome, 365, 1988.

[10] B. Autin, M. Chanel, M. Giovannozzi, M. Martini, *Application of Wigglers to Quasi-Isochronous Transport Systems*, in preparation.

Distribution List

B. Autin	PS/HP
R. Cappi	PS/CA
M. Chanel	PS/CA
J.-P. Delahaye	PS/DR
J. Gareyte	SL/AP
R. Garoby	PS/RF
M. Giovannozzi	PS/CA
H. Haseroth	PS/HP
M. Martini	PS/CA
E. Métral	PS/CA
D. Möhl	PS/DR
J.-P. Riunaud	PS/CA
K. Schindl	PS/DR
H. Schönauer	PS/CA

Filename: open-2000-327
Directory: C:\InetPub\ftproot\convert\in\doc2ps
Template: C:\Documents and Settings\faggianr\Application Data\Microsoft\Templates\Normal.dot
Title: EUROPEAN ORGANIZATION FOR NUCLEAR RESEARCH
Subject:
Author: martinim
Keywords:
Comments:
Creation Date: 1/14/2000 11:05 AM
Change Number: 22
Last Saved On: 12/19/2000 2:10 PM
Last Saved By: faggianr
Total Editing Time: 40 Minutes
Last Printed On: 12/19/2000 2:12 PM
As of Last Complete Printing
Number of Pages: 15
Number of Words: 3,804 (approx.)
Number of Characters: 21,688 (approx.)